J Mater Sci (2006) 41:6789–6799
DOI 10.1007/s10853-006-0207-4

# Modelling off-axis ply matrix cracking in continuous fibre-reinforced polymer matrix composite laminates

**Maria Kashtalyan · Costas Soutis**

Published online: 12 August 2006
© Springer Science+Business Media, LLC 2006

**Abstract** The fracture process of composite laminates subjected to static or fatigue tensile loading involves sequential accumulation of intra- and interlaminar damage, in the form of transverse cracking, splitting and delamination, prior to catastrophic failure. Matrix cracking parallel to the fibres in the off-axis plies is the first damage mode observed. Since a damaged lamina within the laminate retains certain amount of its load-carrying capacity, it is important to predict accurately the stiffness properties of the laminate as a function of damage as well as progression of damage with the strain state. In this paper, theoretical modelling of matrix cracking in the off-axis plies of unbalanced symmetric composite laminates subjected to in-plane tensile loading is presented and discussed. A 2-D shear-lag analysis is used to determine ply stresses in a representative segment and the equivalent laminate concept is applied to derive expressions for Mode I, Mode II and the total strain energy release rate associated with off-axis ply cracking. Dependence of the degraded stiffness properties and strain energy release rates on the crack density and ply orientation angle is examined for glass/epoxy laminates. Suitability of a mixed mode fracture criterion to predict the cracking onset strain is also discussed.

M. Kashtalyan
School of Engineering and Physical Sciences, University of Aberdeen, Fraser Noble Building, Aberdeen AB24 3UE, UK

C. Soutis (✉)
Aerospace Engineering, Faculty of Engineering, The University of Sheffield, Sir Frederick Mappin Building, Mappin Street, Sheffield, S1 3JD, UK
e-mail: c.soutis@sheffield.ac.uk

## Introduction

Interlaminar damage in the form of matrix cracks running parallel to the fibres in off-axis plies of the laminate is the first type of damage observed during the initial stages of the failure process of polymer matrix composite laminates reinforced with continuous fibres. Initiating long before the laminate loses its load-carrying capacity, matrix cracking gradually reduces the stiffness and strength of the laminate [1], changes its coefficients of thermal expansion [2], moisture absorption [3] and the natural frequency [4]. Cracks in the matrix may cause leaks in laminated composite pressure vessels. Matrix cracking triggers development of other, more harmful damage mechanisms, such as delaminations [5] or matrix cracking in the adjacent ply [6–8], or sometimes both. Delamination may result in fibre breakage in the primary load-bearing plies [7] and lead to the loss of the load-carrying capacity of the whole laminate.

Studies of matrix cracking have been focusing predominantly on transverse cracks, i.e., matrix cracks in the 90°-plies of a laminate [9]. The laws of transverse cracking in composite laminates reinforced by glass and carbon fibres are in many respects similar. As a rule, cracks in the matrix occur at equal distances from each other [10] and immediately propagate from edge to edge, cleaving the entire thickness of the damaged ply. Under quasi-static loading, the strain corresponding to the cracking onset decreases with an increased ply thickness [11]. Under cyclic loading, the cycle number corresponding to the beginning of cracking increases with an increased loading amplitude [12]. The degree of transverse cracking is characterized by crack density, i.e., the number of cracks per unit length. After cracking has begun, the crack density abruptly increases with the applied load. The

rate of crack density increase gradually decreases and the matrix cracking comes to saturation state, which is sometimes called a characteristic damaged state. Specifics of transverse cracking of the matrix in $[90_n/0_m]_s$ cross-ply CFRP laminates were studied in [1, 13]. It was established that transverse cracking in the outer 90°-plies begins at lower strains than in the inner plies with a double thickness. However, the saturation crack density is lower in this case. Moreover, cracks are staggered rather than aligned in the outer 90°-plies.

Comprehensive observations of sequential accumulation of matrix cracks in off-axis plies have been reported in the literature, in particular, for carbon/epoxy quasi-isotropic $[0/45/–45/90]_s$ [14] and $[0/90/–45/45]_s$ [15] laminates, carbon/epoxy angle-ply $[0_2/\theta_2/–\theta_2]_s$ laminates [16], as well as glass/epoxy quasi-isotropic $[0/90/–45/45]_s$ laminates [17], glass/epoxy balanced $[45/90]_s$ and $[90/45]_s$ laminates [18], and glass/epoxy angle-ply $[0/\theta/0]$ [19] and $[0/\theta_4/0_{1/2}]_s$ [20] laminates. Longitudinal strain for matrix cracking initiation was found to decrease with increasing ply orientation angle. Also, it was established that ply stresses normal to the fibres at crack formation become progressively smaller as the ply orientation angle increases [21].

The overwhelming majority of studies investigating behaviour and properties of composite laminates with matrix cracks assume that cracks are equally spaced and therefore the analysis can be restricted to a representative segment of the laminate, containing one crack. Stress fields in the cracked off-axis plies were examined by means of finite element method [17, 21] and analytically [22]. Analytical models have been developed to predict stiffness degradation due to off-axis ply cracking in $[\theta]_s$ laminates [23, 24] and quasi-isotropic laminates with matrix cracking in all but 0° layers [25]. Strain energy release rate associated with matrix cracking in the $\theta$-layer of unbalanced symmetric $[0/\theta]_s$ composite laminates was predicted analytically in [26].

The present paper is concerned with theoretical modelling of matrix cracking in off-axis plies of composite laminates subjected to in-plane tensile loading. A 2-D shear-lag analysis is used to determine ply stresses in a representative segment and the equivalent laminate concept is applied to derive expressions for Mode I, Mode II and the total strain energy release rate associated with off-axis ply cracking. Stiffness reduction due to damage and strain energy release rates for off-axis ply cracking in unbalanced symmetric $[0/\theta]_s$ laminates are predicted analytically, and their dependence on the crack density and ply orientation angle is examined for glass/epoxy laminates. Contributions of Mode I and Mode II into the total strain energy rate are identified and then used to predict cracking onset strains in glass/epoxy laminates using a mixed mode fracture criterion.

## Stress analysis

A schematic of an unbalanced symmetric $[0/\theta]_s$ composite laminate with off-axis ply cracks is shown in Fig. 1. The laminate is referred to the global $xyz$ and local $x_1\ x_2\ x_3$ co-ordinate systems, with $x_1$ directed along the fibres in the $\theta$-layer. Matrix cracks are assumed to span the full width of the laminate and full thickness of the $\theta$-layer and be spaced uniformly at a distance $2s$. Due to the periodicity of damage, the stress analysis may be carried out over a representative segment containing one matrix crack. Due to symmetry, it can be further restricted to one quarter of the representative segment, referred to the local co-ordinate system $x_1\ x_2\ x_3$.

Let $\tilde{\sigma}_{ij}^{(k)}$ and $\tilde{\varepsilon}_{ij}^{(k)}$ denote, respectively, the in-plane microstresses and microstrains in the $k$th layer (i.e., stresses and strains averaged across the layer thickness). The in-plane microstresses may be determined by means of a 2-D shear lag analysis. The equilibrium equations in terms of microstresses take the form

$$\frac{\mathrm{d}\tilde{\sigma}_{j2}^{(2)}}{\mathrm{d}x_2} - \frac{\tau_j}{h_2} = 0, \quad j = 1, 2 \tag{1}$$

By averaging the out-of-plane constitutive equations, the interface shear stresses $\tau_j$ in Eq. (1) are expressed in terms of the in-plane displacements $\tilde{u}_{ij}^{(1)}$ and $\tilde{u}_{ij}^{(2)}$, averaged across the thickness of, respectively, outer and inner layers, so that

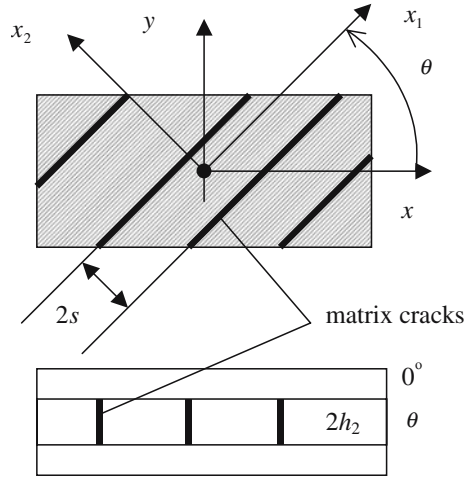


**Fig. 1** Front and edge views of an unbalanced symmetric $[0/\theta]_s$ laminate with off-axis ply cracks

$$\tau_j = K_{j1}(\tilde{u}_1^{(2)} - \tilde{u}_1^{(1)}) + K_{j2}(\tilde{u}_2^{(2)} - \tilde{u}_2^{(1)}) \quad (2)$$

The shear lag parameters $K_{11}$, $K_{22}$ and $K_{12}(\equiv K_{21})$ are determined on the assumption that the out-of-plane shear stresses vary linearly with $x_3$, see Appendix A. Substitution of Eq. (2) into Eq. (1) and subsequent differentiation with respect to $x_2$ lead to the equilibrium equations in terms of in-plane microstresses and microstrains

$$\frac{d^2}{dx_2^2}\tilde{\sigma}_{12}^{(2)} + K_{11}(\tilde{\gamma}_{12}^{(1)} - \tilde{\gamma}_{12}^{(2)}) + K_{12}(\tilde{\varepsilon}_{22}^{(1)} - \tilde{\varepsilon}_{22}^{(2)}) = 0 \quad (3a)$$

$$\frac{d^2}{dx_2^2}\tilde{\sigma}_{22}^{(2)} + K_{21}(\tilde{\gamma}_{12}^{(1)} - \tilde{\gamma}_{12}^{(2)}) + K_{22}(\tilde{\varepsilon}_{22}^{(1)} - \tilde{\varepsilon}_{22}^{(2)}) = 0 \quad (3b)$$

To exclude the microstrains, constitutive equations for both layers are employed

$$\begin{Bmatrix} \tilde{\sigma}_{11}^{(1)} \\ \tilde{\sigma}_{22}^{(1)} \\ \tilde{\sigma}_{12}^{(1)} \end{Bmatrix} = \begin{bmatrix} \hat{Q}_{11}^{(1)} & \hat{Q}_{12}^{(1)} & \hat{Q}_{16}^{(1)} \\ \hat{Q}_{12}^{(1)} & \hat{Q}_{22}^{(1)} & \hat{Q}_{26}^{(1)} \\ \hat{Q}_{16}^{(1)} & \hat{Q}_{26}^{(1)} & \hat{Q}_{66}^{(1)} \end{bmatrix} \begin{Bmatrix} \tilde{\varepsilon}_{11}^{(1)} \\ \tilde{\varepsilon}_{22}^{(1)} \\ \tilde{\gamma}_{12}^{(1)} \end{Bmatrix}$$

$$\begin{Bmatrix} \tilde{\sigma}_{11}^{(2)} \\ \tilde{\sigma}_{22}^{(2)} \\ \tilde{\sigma}_{12}^{(2)} \end{Bmatrix} = \begin{bmatrix} \hat{Q}_{11}^{(2)} & \hat{Q}_{12}^{(2)} & 0 \\ \hat{Q}_{12}^{(2)} & \hat{Q}_{22}^{(2)} & 0 \\ 0 & 0 & \hat{Q}_{66}^{(2)} \end{bmatrix} \begin{Bmatrix} \tilde{\varepsilon}_{11}^{(2)} \\ \tilde{\varepsilon}_{22}^{(2)} \\ \tilde{\gamma}_{12}^{(2)} \end{Bmatrix} \quad (4)$$

as well as the generalised plane strain condition $\tilde{\varepsilon}_{11}^{(1)} = \tilde{\varepsilon}_{11}^{(2)}$ and equations of the global equilibrium of the laminate

$$h_1 \begin{Bmatrix} \tilde{\sigma}_{11}^{(1)} \\ \tilde{\sigma}_{22}^{(1)} \\ \tilde{\sigma}_{12}^{(1)} \end{Bmatrix} + h_2 \begin{Bmatrix} \tilde{\sigma}_{11}^{(2)} \\ \tilde{\sigma}_{22}^{(2)} \\ \tilde{\sigma}_{12}^{(2)} \end{Bmatrix} = (h_1 + h_2)\bar{\sigma}_x \begin{Bmatrix} \cos^2\theta \\ \sin^2\theta \\ -\cos\theta\sin\theta \end{Bmatrix} \quad (5)$$

Finally, a system of coupled second order non-homogeneous ordinary differential equations is obtained (see Appendix B), solutions to which are

$$\tilde{\sigma}_{j2}^{(2)} = \left( \sum_{k=1}^{2} A_{kj} \frac{\cosh \lambda_k (x_2 - s)}{\cosh \lambda_k s} + C_j \right) \bar{\sigma}_x, \quad (6)$$

Here $\bar{\sigma}_x$ is the applied stress, $\lambda_k$ are the roots of the characteristic equation, and $A_{kj}$ and $C_j$ ($j$ = 1,2) are constants depending on the in-plane stiffness properties $[\hat{Q}^{(1)}]$, $[\hat{Q}^{(2)}]$ of the intact material of the layers, shear lag parameters $K_{11}$, $K_{22}$ and $K_{12}$ and angle $\theta$.

## Stiffness analysis

The in-plane microstresses in the damaged layer can be used to evaluate the reduction of the laminate stiffness properties due to damage. Instead of the damaged laminate one considers an ECM laminate, in which the damaged ply is replaced with an equivalent homogeneous layer with degraded stiffness properties. The constitutive equations of the 'equivalent' layer are

$$\{\bar{\sigma}^{(2)}\} = [\bar{Q}^{(2)}]\{\bar{\varepsilon}^{(2)}\} \quad (7)$$

The lamina macrostresses $\{\bar{\sigma}^{(2)}\}$, involved in Eq. (7), are obtained by averaging the microstresses, Eq. (6), across the length of the representative segment as explicit functions of the relative crack density $D^{mc}=h_2/s$

$$\bar{\sigma}_{j2}^{(2)} = \left( \sum_{k=1}^{2} A_{kj} \frac{D^{mc}}{\lambda_k h_2} \tanh \frac{\lambda_k h_2}{D^{mc}} + C_j \right) \bar{\sigma}_x, \quad j = 1, 2 \quad (8)$$

The macrostrains in the equivalent layer $\{\bar{\varepsilon}^{(2)}\}$ are calculated from the constitutive equations for both layers, Eq. (4), and equations of the global equilibrium of the laminate, Eq. (5), assuming $\{\bar{\varepsilon}^{(2)}\} = \{\bar{\varepsilon}^{(1)}\}$.

The in-plane stiffness matrix $[\bar{Q}^{(2)}]$ of the equivalent homogeneous layer in the local co-ordinate system is related to the in-plane stiffness matrix $[\hat{Q}^{(2)}]$ of the undamaged material via the In-situ Damage Effective Functions (IDEFs) [27] $\Lambda_{jj}=\Lambda_{jj}(D^{mc})$, $j$=2,6 as

$$[\bar{Q}^{(2)}] = [\hat{Q}^{(2)}] - \begin{bmatrix} (\hat{Q}_{12}^{(2)})^2/\hat{Q}_{22}^{(2)}\Lambda_{22} & \hat{Q}_{12}^{(2)}\Lambda_{22} & 0 \\ \hat{Q}_{12}^{(2)}\Lambda_{22} & \hat{Q}_{22}^{(2)}\Lambda_{22} & 0 \\ 0 & 0 & \hat{Q}_{66}^{(2)}\Lambda_{66} \end{bmatrix} \quad (9)$$

Substituting Eq. (9) into the constitutive equations for the 'equivalent' layer, Eq. (7), gives the IDEFs $\Lambda_{22}$, $\Lambda_{66}$ in terms of the lamina macrostresses $\{\bar{\sigma}^{(2)}\}$ and macrostrains $\{\bar{\varepsilon}^{(2)}\}$ as

$$\Lambda_{22} = 1 - \frac{\bar{\sigma}_{22}^{(2)}}{\hat{Q}_{12}^{(2)}\bar{\varepsilon}_{11}^{(2)} + \hat{Q}_{22}^{(2)}\bar{\varepsilon}_{22}^{(2)}}, \quad \Lambda_{66} = 1 - \frac{\bar{\sigma}_{12}^{(2)}}{\hat{Q}_{66}^{(2)}\bar{\gamma}_{12}^{(2)}} \quad (10)$$

The in-plane stiffness matrix $[\bar{Q}]_2$ of the 'equivalent' layer in the global co-ordinate system $xyz$ (Fig. 1) can be obtained from the in-plane stiffness matrix $[\bar{Q}^{(2)}]$ in the local co-ordinate system $x_1\ x_2\ x_3$ by the well-known transformation formulae [28].

## Fracture analysis

The total strain energy release rate $G^{\mathrm{mc}}$ associated with matrix cracking in the $\theta$-layer of the $[0/\theta]_s$ laminate is equal to the first partial derivative of the total strain energy $U$ stored in the damaged laminate with respect to the total area covered by cracks provided the applied strains $\{\bar{\varepsilon}\}$ are fixed

$$G^{\mathrm{mc}} = -\left.\frac{\partial U}{\partial A^{\mathrm{mc}}}\right|_{\{\bar{\varepsilon}\}} \tag{11}$$

In the global co-ordinates, the total strain energy stored in the laminate element with a finite gauge length $L$ and width $w$ is

$$\begin{aligned} U = \frac{wL}{2}\sum_k (z_k - z_{k-1})(\{\bar{\varepsilon}\} + \{\bar{\varepsilon}_k^{\mathrm{thermal}}\} \\ + \{\bar{\varepsilon}_k^{\mathrm{hygro}}\})^{\mathrm{T}}[\bar{Q}]_k(\{\bar{\varepsilon}\} + \{\bar{\varepsilon}_k^{\mathrm{thermal}}\} + \{\bar{\varepsilon}_k^{\mathrm{hygro}}\}) \end{aligned} \tag{12}$$

where $\{\bar{\varepsilon}_k^{\mathrm{thermal}}\}$and $\{\bar{\varepsilon}_k^{\mathrm{hygro}}\}$ are, respectively, residual thermal and residual hygroscopic strains in the laminate due to the temperature and moisture difference between the stress-free and actual state, and $[\bar{Q}]_k$ is the in-plane reduced stiffness matrix of layer $k$ in the global co-ordinates.

Since the area of a single crack is equal to $a^{\mathrm{mc}}=2h_2\ w/|\sin\theta|$, the total area covered by all cracks is equal to

$$A^{\mathrm{mc}} = a^{\mathrm{mc}}C^{\mathrm{mc}}L = LwD^{\mathrm{mc}}/|\sin\theta| \tag{13}$$

If hygrothermal effects are neglected, the strain energy releases rate for matrix cracking, calculated from Eq. (11) to Eq. (13), is

$$G^{\mathrm{mc}}(\bar{\varepsilon},\ D^{\mathrm{mc}}) = -h_2\{\bar{\varepsilon}\}^{\mathrm{T}}\frac{\partial[\bar{Q}]_2}{\partial D^{\mathrm{mc}}}\{\bar{\varepsilon}\}|\sin\theta| \tag{14}$$

Under uniaxial strain, Eq. (14) simplifies to

$$G^{\mathrm{mc}}(\bar{\varepsilon}_{xx},\ D^{\mathrm{mc}}) = -h_2\bar{\varepsilon}_{xx}^2\frac{\partial\bar{Q}_{xx,2}}{\partial D^{\mathrm{mc}}}|\sin\theta| \tag{15}$$

Calculation of the in-plane axial stiffness $\bar{Q}_{xx,2}$ using Eq. (9) and the transformation formulae [28], yields the strain energy release rate for off-axis ply cracking in terms of the In-situ Damage Effective Functions (IDEFs) $\Lambda_{22}$, $\Lambda_{66}$ and stiffness properties of the undamaged material $\hat{Q}_{ij}^{(2)}$ as follows:

$$\begin{aligned} &G^{\mathrm{mc}}(\bar{\varepsilon}_{xx}, D^{\mathrm{mc}}) \\ &= h_2\bar{\varepsilon}_{xx}^2\left[\left(\frac{\hat{Q}_{12}^{(2)2}}{\hat{Q}_{22}^{(2)}}\cos^4\theta + 2\hat{Q}_{12}^{(2)}\sin^2\theta\cos^2\theta + + \hat{Q}_{22}^{(2)}\sin^4\theta\right)\right. \\ &\qquad\left.\times\frac{\partial\Lambda_{22}}{\partial D^{\mathrm{mc}}} + 4\hat{Q}_{66}^{(2)}\sin^2\theta\cos^2\theta\frac{\partial\Lambda_{66}}{\partial D^{\mathrm{mc}}}\right]|\sin\theta| \end{aligned} \tag{16}$$

The first partial derivatives of IDEFs that appear in Eq. (16) are explicit functions of the relative crack density $D^{\mathrm{mc}}$ and can be calculated analytically.

Even under the uniaxial loading, damage development in the off-axis plies of general symmetric laminates always occurs under mixed mode conditions due to shear-extension coupling. It is, therefore, important in the calculation of the total strain energy release rate to be able to separate Mode I and Mode II contributions.

For a $[0/\theta]_s$ laminate with damaged $\theta$-layer modelled by an 'equivalent' laminate, the total strain energy release rate for off-axis ply cracking is equal to the first partial derivative of the portion of the total strain energy stored in the equivalent homogeneous layer with respect to damage area

$$G^{\mathrm{mc}} = -\left.\frac{\partial U^{(2)}}{\partial A^{\mathrm{mc}}}\right|_{\{\bar{\varepsilon}\}} \tag{17}$$

In the local co-ordinates (Fig. 1), this portion of the total strain energy can be separated into extensional and shear parts

$$\begin{aligned} U^{(2)} = U_{\mathrm{I}}^{(2)} + U_{\mathrm{II}}^{(2)} = Lwh_2(\bar{\sigma}_{11}^{(2)}\bar{\varepsilon}_{11}^{(2)} + \bar{\sigma}_{22}^{(2)}\bar{\varepsilon}_{22}^{(2)}) \\ + Lwh_2\bar{\sigma}_{12}^{(2)}\bar{\gamma}_{12}^{(2)} \end{aligned} \tag{18}$$

Under uniaxial strain $\bar{\varepsilon}_{xx}$, strains and stresses in the 'equivalent' homogeneous layer are

$$\begin{aligned} \{\bar{\varepsilon}^{(2)}\} &= \{\cos^2\theta,\ \sin^2\theta,\ 2\cos\theta\sin\theta\}^{\mathrm{T}}\bar{\varepsilon}_{xx}, \\ \{\bar{\sigma}^{(2)}\} &= [Q^{(2)}]\{\cos^2\theta,\ \sin^2\theta,\ 2\cos\theta\sin\theta\}^{\mathrm{T}}\bar{\varepsilon}_{xx} \end{aligned} \tag{19}$$

where the modified stiffness matrix $[Q^{(2)}]$ of the equivalent homogeneous layer in the local co-ordinates is given by Eq. (9). Substitution of Eqs. (13), (18) and (19) into Eq. (17) gives Mode I and Mode II contributions into the total strain energy release rate for off-axis ply cracking

$$G_{\mathrm{I}}^{\mathrm{mc}} = -\frac{\partial U_{\mathrm{I}}^{(2)}}{\partial A^{\mathrm{mc}}} = \bar{\varepsilon}_{xx}^{2} f_{1}^{\mathrm{mc}}(D^{\mathrm{mc}}) \tag{20a}$$

$$f_{1}^{\mathrm{mc}}(D^{\mathrm{mc}}) = h_2 \left( \frac{\hat{Q}_{12}^{(2)2}}{\hat{Q}_{22}^{(2)}} \cos^4\theta + 2\hat{Q}_{12}^{(2)} \sin^2\theta \cos^2\theta + \hat{Q}_{22}^{(2)} \sin^4\theta \right) \frac{\partial \Lambda_{22}}{\partial D^{\mathrm{mc}}} |\sin\theta| \tag{20b}$$

$$G_{\mathrm{II}}^{\mathrm{mc}} = -\frac{\partial U_{II}^{(2)}}{\partial A^{\mathrm{mc}}} = \bar{\varepsilon}_{xx}^{2} f_{2}^{\mathrm{mc}}(D^{\mathrm{mc}}) \tag{21a}$$

$$f_{2}^{\mathrm{mc}}(D^{\mathrm{mc}}) = 4h_2 \hat{Q}_{66}^{(2)} \frac{\partial \Lambda_{66}}{\partial D^{\mathrm{mc}}} \cos^2\theta |\sin^3\theta| \tag{21b}$$

These expressions can be used with appropriate fracture criteria to estimate the onset of matrix cracking in the off-axis plies. The resulting total strain energy release rate $G^{\mathrm{mc}}=G_{\mathrm{I}}^{\mathrm{mc}}+G_{\mathrm{II}}^{\mathrm{mc}}$ coincides with Eq. (16).

## Results and discussion

To validate the developed approach, a case of $[30/90]_s$ laminate with matrix cracks in the 90°-ply was considered, and the results were compared to predictions made using the generalised plane strain model [29]. The properties of a unidirectional glass/epoxy material system used in the calculations were as follows: ply thickness 0.25 mm, longitudinal Young's modulus $E_A$ =45.6 GPa, transverse Young's modulus $E_T$ = 16.2 GPa, in-plane shear modulus $\mu_A$=5.83 GPa, major Poisson's ratio $\nu_A$ = 0.278, minor Poisson's ratio $\nu_T$ =0.4. From the laminated plate theory [28] stiffness properties of the intact $[30/90]_s$ laminate are calculated as follows: axial modulus $\hat{E}_x = 20.9$ GPa, transverse modulus $\hat{E}_y =$ 30.4 GPa, in-plane shear modulus $\hat{G}_{xy} = 7.76$ GPa, major Poisson's ratio $\hat{\nu}_x = 0.2$, axial and transverse shear-extension coupling coefficients $\eta_{xy,x}$ = –0.53, $\eta_{xy,y}$ = –0.014, respectively. Table 1 shows reduction of the laminate's stiffness properties as a function of a crack density in the 90°-ply. As one would expect, the present shear lag-based model predicts slightly bigger stiffness reduction than the generalised plane strain approach used in combination with ply refinement technique. For the axial Young's modulus the difference is within 4.1%, for shear modulus within 7.2%, for Poisson's ratio within 3.9%, and for axial and transverse shear-extension coupling coefficients within 5.3% and 3.4%, respectively. It is anticipated that the difference between two approached would be smaller if lower levels of ply refinement are used in the generalised plane strain model [29].

**Table 1** Stiffness properties of a $[30/90]_s$ glass/epoxy cracked laminate

| Crack density (crack/cm) | Present model | McCartney's model [29] | Difference (%) |
|---|---|---|---|
| *Axial Young's modulus* | | | |
| 0 | 20.93 | 20.9287 | 0.0% |
| 5 | 17.82 | 18.0412 | –1.2% |
| 10 | 15.68 | 15.9644 | –1.8% |
| 15 | 14.41 | 14.7812 | –2.5% |
| 20 | 13.67 | 14.1276 | –3.2% |
| 25 | 13.22 | 13.7295 | –3.7% |
| 30 | 12.93 | 13.4625 | –4.0% |
| 35 | 12.73 | 13.2697 | –4.1% |
| 40 | 12.6 | 13.1231 | –4.0% |
| *Shear modulus* | | | |
| 0 | 7.756 | 7.7565 | 0.0% |
| 5 | 6.807 | 7.0439 | –3.4% |
| 10 | 6.157 | 6.4582 | –4.7% |
| 15 | 5.668 | 6.0115 | –5.7% |
| 20 | 5.315 | 5.6882 | –6.6% |
| 25 | 5.071 | 5.4546 | –7.0% |
| 30 | 4.902 | 5.2831 | –7.2% |
| 35 | 4.782 | 5.1543 | –7.2% |
| 40 | 4.697 | 5.0551 | –7.1% |
| *Poisson's ratio* | | | |
| 0 | 0.2049 | 0.2049 | 0.0% |
| 5 | 0.1762 | 0.1782 | –1.1% |
| 10 | 0.1564 | 0.1591 | –1.7% |
| 15 | 0.1445 | 0.1481 | –2.4% |
| 20 | 0.1375 | 0.1419 | –3.1% |
| 25 | 0.1332 | 0.1382 | –3.6% |
| 30 | 0.1305 | 0.1356 | –3.8% |
| 35 | 0.1286 | 0.1338 | –3.9% |
| 40 | 0.1273 | 0.1324 | –3.9% |
| *Axial shear-extension coupling coefficient* | | | |
| 0 | –0.5292 | –0.5292 | 0.0% |
| 5 | –0.5889 | –0.5791 | 1.7% |
| 10 | –0.6354 | –0.6179 | 2.8% |
| 15 | –0.6753 | –0.65 | 3.9% |
| 20 | –0.7078 | –0.676 | 4.7% |
| 25 | –0.7325 | –0.6966 | 5.2% |
| 30 | –0.7508 | –0.7129 | 5.3% |
| 35 | –0.7643 | –0.7257 | 5.3% |
| 40 | –0.7743 | –0.7359 | 5.2% |
| *Transverse shear-extension coupling coefficient* | | | |
| 0 | –0.009838 | –0.0098 | 0.4% |
| 5 | –0.008167 | –0.0079 | 3.4% |
| 10 | –0.006807 | –0.0066 | 3.1% |
| 15 | –0.00604 | –0.0059 | 2.4% |
| 20 | –0.005657 | –0.0056 | 1.0% |
| 25 | –0.005458 | –0.0055 | –0.8% |
| 30 | –0.005348 | –0.0054 | –1.0% |
| 35 | –0.005283 | –0.0054 | –2.2% |
| 40 | –0.005241 | –0.0053 | –1.1% |

Reduction of the laminate's stiffness properties with the crack density $C^{\mathrm{mc}} = (2s)^{-1}$ in $[0/\theta]_s$ glass/epoxy laminates is shown in Fig. 2 for four ply orientation angles $\theta$: 45°, 60°, 75° and 90°. The plotted values represent normalised (i.e.,

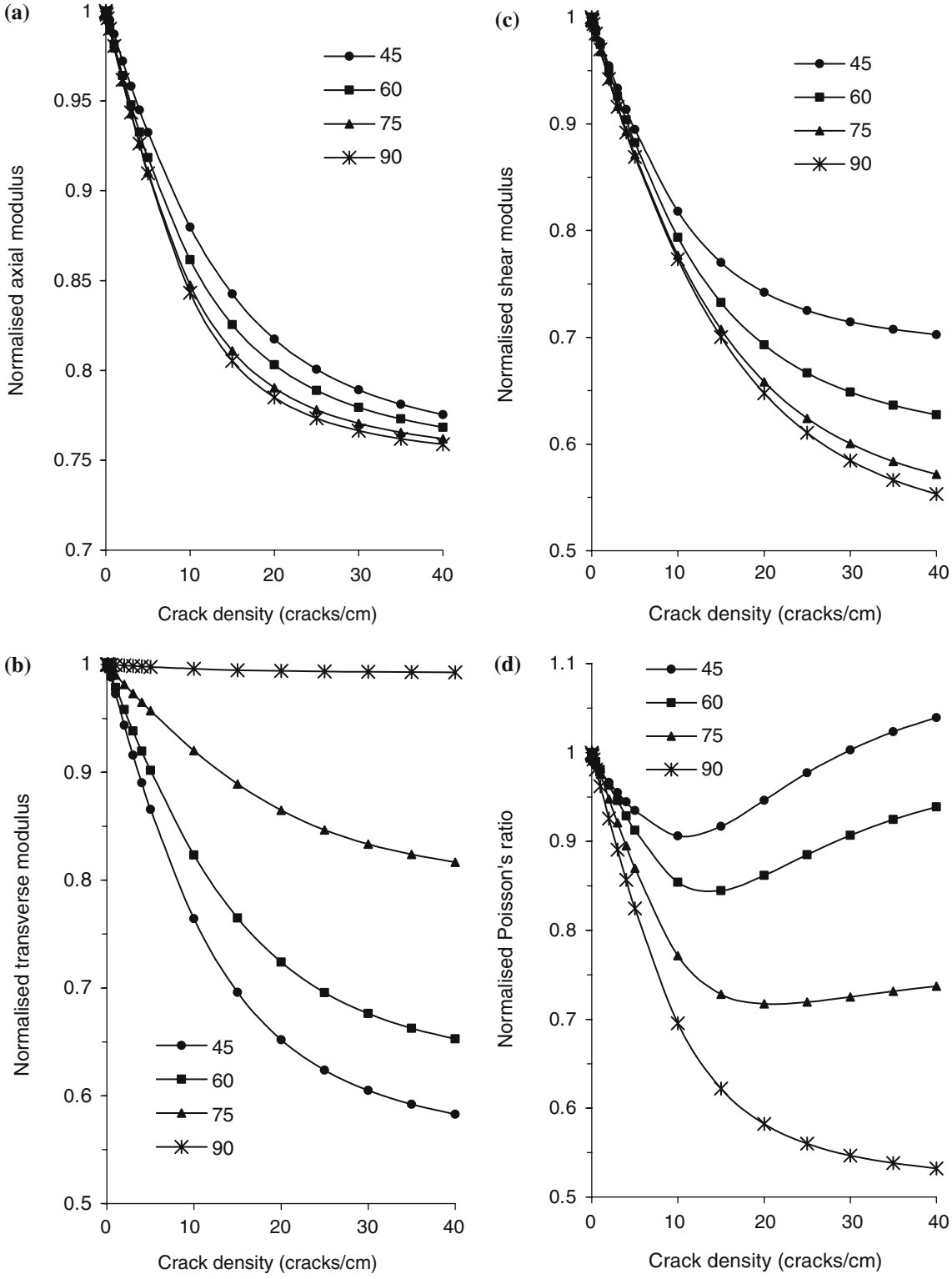


**Fig. 2** Normalised stiffness properties of $[0_2/\theta_2]_s$ glass/epoxy laminates as a function of crack density $C^{mc}$ in the inner $\theta$-layer (cracks/cm): (**a**) axial modulus; (**b**) transverse modulus; (**c**) shear modulus; (**d**) major Poisson's ratio

referred to their values in the undamaged state) axial modulus $E_x/\hat{E}_x$ (Fig. 2a), transverse modulus $E_y/\hat{E}_y$ (Fig.2b), in-plane shear modulus $G_{xy}/\hat{G}_{xy}$ (Fig.2c) and major Poisson's ratio $v_{xy}/\hat{v}_{xy}$ (Fig. 2d). It may be seen that the most significantly reduced properties are transverse and shear moduli. While in cross-ply $[0/90]_s$ laminates the

Poisson's ratio decreases monotonously with the crack density, this is not the case for other ply orientation angles (Fig. 2d).

Unbalanced angle-ply laminates, such as $[0/\theta]_s$ lay-up, exhibit shear extension coupling characterised by axial $\eta_{xy,x} = \bar{\gamma}_{xy}/\bar{\varepsilon}_x$ and transverse $\eta_{xy,y} = \bar{\gamma}_{xy}/\bar{\varepsilon}_y$ shear-extension coefficients. Figure 3 shows variation of the shear-extension coupling coefficients with the crack density $C^{\mathrm{mc}}$ in $[0/\theta]_s$ glass/epoxy laminates for the same range of ply orientation angles $\theta$. It may be seen that for some ply orientation angles, matrix cracking in the off-axis ply can significantly increase shear-extension coupling.

Glass/epoxy angle-ply laminates exhibit significantly higher levels of normalised strain energy release rates for matrix cracking than carbon/epoxy ones [22]. Figure 4 shows Mode I (Fig.4a) and Mode II (Fig. 4b) contributions as well as the total normalised strain energy release rate $G^{\mathrm{mc}}/\bar{\varepsilon}_{xx}^2$ (Fig. 4c) associated with matrix cracking in glass/epoxy $[0/\theta]_s$ laminates as a function of crack density $C^{\mathrm{mc}}$ for four ply orientation angles: 45°, 60°, 75° and 90°. As the ply orientation angle increases, Mode I contribution into the total energy release rate increases, too (Fig. 4a), while Mode II contribution decreases (Fig. 4b) becoming zero in the case of a cross-ply $[0/90]_s$ laminate.

To predict the development of the off-axis ply cracks in the $\theta$-layer of a $[0/\theta]_s$ laminate, it is suggested to use a mixed mode fracture criterion

$$\left(\frac{G_{\mathrm{I}}}{G_{\mathrm{IC}}}\right)^M + \left(\frac{G_{\mathrm{II}}}{G_{\mathrm{IIC}}}\right)^N = 1 \tag{22}$$

where $G_{\mathrm{IC}}$ and $G_{\mathrm{IIC}}$ are, respectively, Mode I and Mode II interlaminar fracture toughnesses. The exponents $M$ and $N$ depend on the material system. Following [30], we take them for a glass/epoxy system as $M = 1$, $N = 2$.

Predicted cracking onset strains for $[0/\theta]_s$ glass/epoxy laminates are shown in Fig. 5 together with experimentally obtained data for specimens with as-cut, polished and notched edges [19]. To predict cracking onset strains, $G_{\mathrm{I}}^{\mathrm{mc}}$ and $G_{\mathrm{II}}^{\mathrm{mc}}$ values are calculated from Eqs. (20) and (21), and cracking onset strain $\bar{\varepsilon}_{xx}$ is found as a root of the following equation

$$\bar{\varepsilon}_{xx}^4 \left(\frac{f_2(D^{\mathrm{mc}})}{G_{\mathrm{IIC}}}\right)^2 + \bar{\varepsilon}_{xx}^2 \left(\frac{f_1(D^{\mathrm{mc}})}{G_{\mathrm{IC}}}\right) = 1 \quad \text{when} \quad D^{\mathrm{mc}} \to 0 \tag{23}$$

Since for the considered glass/epoxy system the exact $G_{\mathrm{IC}}$ and $G_{\mathrm{IIC}}$ critical values are unknown, predictions are made using typical for glass/epoxy systems values of $G_{\mathrm{IC}}$ =200 J/m$^2$ and $G_{\mathrm{IIC}}$ = 1500 J/m$^2$.

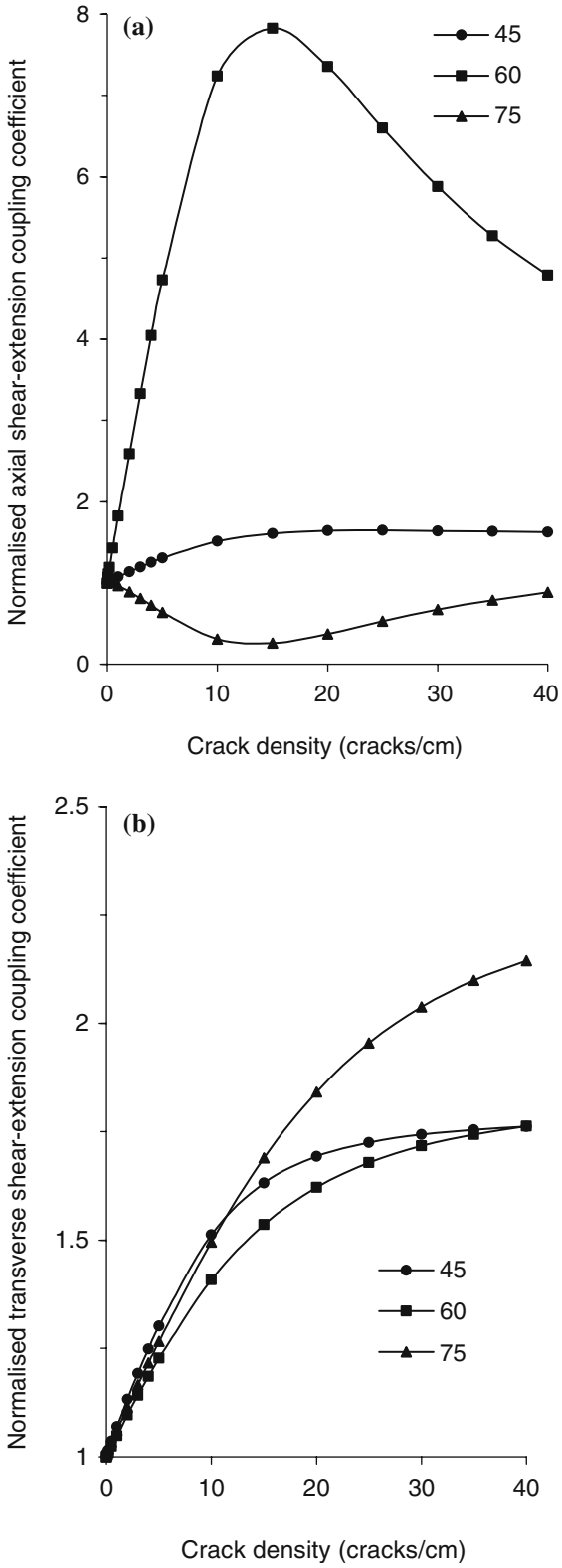


**Fig. 3** Shear extension coupling coefficients of a $[0_2/\theta_2]_s$ glass/epoxy laminates as a function of crack density $C^{\mathrm{mc}}$ in the inner layer (cracks/cm): (**a**) axial; (**b**) transverse

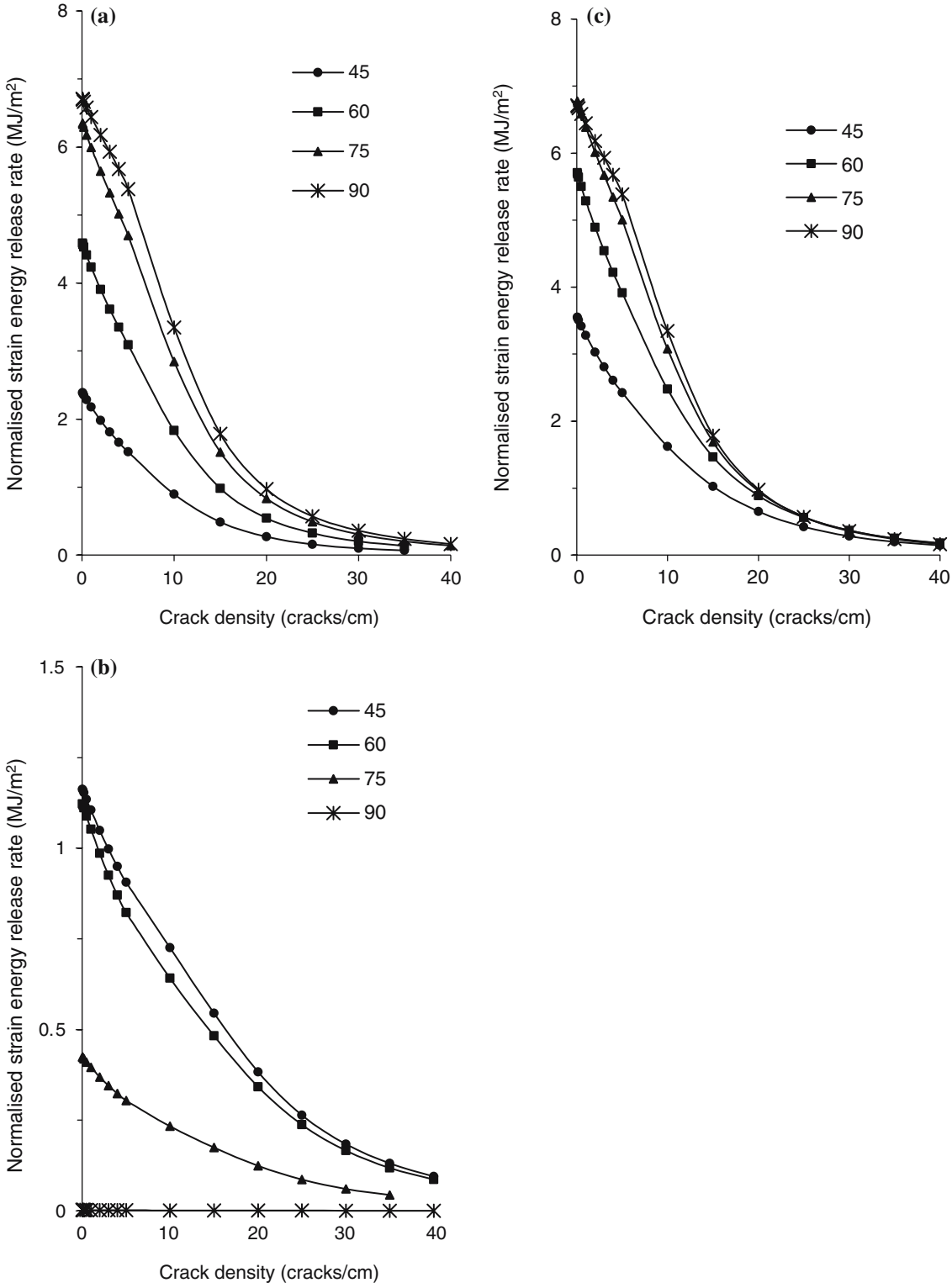


**Fig. 4** Normalised strain energy release rate $G^{mc}/\bar{\varepsilon}_{xx}^2$ for matrix cracking in a $[0/\theta]_s$ glass/epoxy laminate as a function of crack density $C^{mc}$ in the inner $\theta$-layer (cracks/cm): (**a**) Mode I contribution; (**b**) Mode II contribution; (**c**) total

Comparison with limited experimental data shows that the mixed mode fracture criterion, Eq. (22), can successfully predict the initiation of matrix cracking for ply orientation angles $75° \leq \theta \leq 90°$. For $45° \leq \theta \leq 75°$, measured strains are much higher than predictions. Also, they increase steeply as $\theta$ decreases.

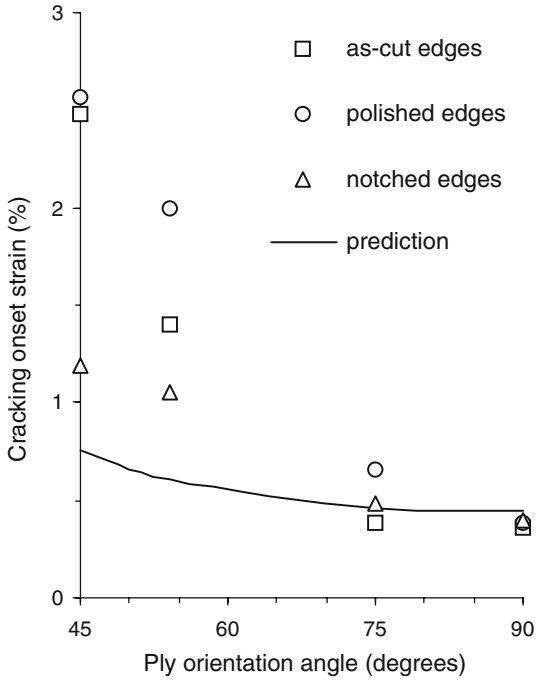


**Fig. 5** Off-axis ply cracking onset strain as a function of ply orientation angle $\theta$ in glass/epoxy $[0/\theta]_s$ laminates

Further work is required to develop an appropriate fracture or failure criterion that captures initiation and development of matrix cracks in off-axis plies of composite laminates reinforced by glass or carbon fibres, especially for $\theta < 75°$.

## Conclusions

Matrix cracks parallel to the fibres in the off-axis plies is the first intralaminar damage mode observed in laminated composites subjected to static or fatigue in-plane tensile loading. They reduce laminate stiffness and strength and trigger development of other damage modes, such as delaminations. This paper is concerned with theoretical modelling of continuous fibre-reinforced polymer matrix composite laminates with off-axis ply cracks. Closed-form analytical expressions are derived for Mode I, Mode II and the total strain energy release rates associated with off-axis ply cracking in $[0/\theta]_s$ laminates, representing them as linear functions of the first partial derivatives of the effective elastic properties of the damaged layer with respect to appropriate damage parameters. These expressions can be used with appropriate fracture criteria to estimate the onset and growth of damage in off-axis plies.

As far as stiffness reduction induced by matrix cracking is concerned, the laminate axial and transverse moduli of angle-ply laminates are reduced more significantly than respective stiffness properties of cross-ply laminates, while for the shear modulus, the opposite is true. Matrix cracking in the off-axis plies can also result in an increase in the Poisson's ratio of the laminate.

**Acknowledgements** Financial support of this research by Engineering and Physical Sciences Research Council (EPSRC/GR/L51348 and EPSRC/GR/A31001/02) and the British Ministry of Defence is gratefully acknowledged. The authors would like to thank Dr LN McCartney for helpful discussions, and also for providing his numerical results for comparison purposes.

## Appendix A

Variation of the out-of-plane shear stresses has the form

$$\begin{aligned} &\sigma_{j3}^{(2)} = \frac{\tau_j}{h_2} x_3, \quad 0 \leqslant |x_3| \leqslant h_2, \\ &j = 1,2, \quad \sigma_{j3}^{(1)} = \frac{\tau_j}{h_1}(h - x_3), \quad h_2 \leqslant |x_3| \leqslant h \end{aligned} \tag{24}$$

Constitutive equations for the out-of-plane shear stresses are

$$\begin{Bmatrix} \sigma_{13}^{(k)} \\ \sigma_{23}^{(k)} \end{Bmatrix} \approx \begin{bmatrix} Q_{55}^{(k)} & Q_{45}^{(k)} \\ Q_{45}^{(k)} & Q_{44}^{(k)} \end{bmatrix} \frac{\partial}{\partial x_3} \begin{Bmatrix} u_1^{(k)} \\ u_2^{(k)} \end{Bmatrix}, \quad i = 1,2 \tag{25}$$

After substituting Eq. (25) into Eq. (24), multiplying them by $x_3$ and by $h$–$x_3$ respectively and integrating with respect to $x_3$ we get

$$\frac{h_1}{3} \begin{Bmatrix} \tau_1 \\ \tau_2 \end{Bmatrix} = \begin{bmatrix} \hat{Q}_{55}^{(1)} & \hat{Q}_{45}^{(1)} \\ \hat{Q}_{45}^{(1)} & \hat{Q}_{44}^{(1)} \end{bmatrix} \left( \begin{Bmatrix} \tilde{u}_1^{(1)} \\ \tilde{u}_2^{(1)} \end{Bmatrix} - \begin{Bmatrix} U_1 \\ U_2 \end{Bmatrix} \right) \tag{26a}$$

$$\frac{h_2}{3} \begin{Bmatrix} \tau_1 \\ \tau_2 \end{Bmatrix} = \begin{bmatrix} \hat{Q}_{55}^{(2)} & \hat{Q}_{45}^{(2)} \\ \hat{Q}_{45}^{(2)} & \hat{Q}_{44}^{(2)} \end{bmatrix} \left( \begin{Bmatrix} U_1 \\ U_2 \end{Bmatrix} - \begin{Bmatrix} \tilde{u}_1^{(2)} \\ \tilde{u}_2^{(2)} \end{Bmatrix} \right) \tag{26b}$$

Here $\{U_j\} = \{u_j^{(1)}\}|_{x\_3 = h\_2} = \{u_j^{(2)}\}|_{x\_3 = h\_2}$, $j$=1,2 are the in-plane displacements at the interface. After rearranging Eqs. (26a) and (26b) become

$$\begin{aligned} \begin{Bmatrix} \tilde{u}_1^{(1)} \\ \tilde{u}_2^{(1)} \end{Bmatrix} - \begin{Bmatrix} \tilde{u}_1^{(2)} \\ \tilde{u}_2^{(2)} \end{Bmatrix} = \Bigg( &\frac{h_1}{3} \begin{bmatrix} \hat{Q}_{55}^{(1)} & \hat{Q}_{45}^{(1)} \\ \hat{Q}_{45}^{(1)} & \hat{Q}_{44}^{(1)} \end{bmatrix}^{-1} \\ &+ \frac{h_2}{3} \begin{bmatrix} \hat{Q}_{55}^{(2)} & \hat{Q}_{45}^{(2)} \\ \hat{Q}_{45}^{(2)} & \hat{Q}_{44}^{(2)} \end{bmatrix}^{-1} \Bigg) \begin{Bmatrix} \tau_1 \\ \tau_2 \end{Bmatrix} \end{aligned} \tag{27}$$

Inversion of Eq. (27) leads to

$$\left\{ \begin{matrix} \tau_1 \\ \tau_2 \end{matrix} \right\} = \begin{bmatrix} K_{11} & K_{12} \\ K_{21} & K_{22} \end{bmatrix} \left( \left\{ \begin{matrix} \tilde{u}_1^{(1)} \\ \tilde{u}_2^{(1)} \end{matrix} \right\} - \left\{ \begin{matrix} \tilde{u}_1^{(2)} \\ \tilde{u}_2^{(2)} \end{matrix} \right\} \right), \tag{28a}$$

$$\begin{bmatrix} K_{11} & K_{12} \\ K_{21} & K_{22} \end{bmatrix} = \left( \frac{h_1}{3} \begin{bmatrix} \hat{Q}_{55}^{(1)} & \hat{Q}_{45}^{(1)} \\ \hat{Q}_{45}^{(1)} & \hat{Q}_{44}^{(1)} \end{bmatrix}^{-1} + \frac{h_2}{3} \begin{bmatrix} \hat{Q}_{55}^{(2)} & \hat{Q}_{45}^{(2)} \\ \hat{Q}_{45}^{(2)} & \hat{Q}_{44}^{(2)} \end{bmatrix}^{-1} \right)^{-1} \tag{28b}$$

## Appendix B

On applying the constitutive equations, inverse to Eq. (4), the generalised plane strain condition $\tilde{\varepsilon}_{11}^{(1)} = \tilde{\varepsilon}_{11}^{(2)}$ becomes

$$S_{11}^{(1)}\tilde{\sigma}_{11}^{(1)} + S_{12}^{(1)}\tilde{\sigma}_{22}^{(1)} + S_{16}^{(1)}\tilde{\sigma}_{12}^{(1)} = \hat{S}_{11}^{(2)}\tilde{\sigma}_{11}^{(2)} + \hat{S}_{12}^{(2)}\tilde{\sigma}_{22}^{(2)} \tag{29}$$

where $\hat{S}_{ij}^{(k)}$ are the compliances for the $k$th layer. Using the laminate equilibrium equations, Eq. (5), stresses in the 1st layer can be excluded, so that

$$\tilde{\sigma}_{11}^{(2)} = a_{22}\tilde{\sigma}_{22}^{(2)} + a_{12}\tilde{\sigma}_{12}^{(2)} + b\bar{\sigma}_x, \tag{30}$$

$$a_{22} = -\frac{\hat{S}_{12}^{(1)} + \chi\hat{S}_{12}^{(2)}}{\hat{S}_{11}^{(1)} + \chi\hat{S}_{11}^{(2)}}, \quad a_{12} = -\frac{\hat{S}_{16}^{(1)}}{\hat{S}_{11}^{(1)} + \chi\hat{S}_{11}^{(2)}}, \quad \chi = \frac{h_1}{h_2},$$

$$b = (1+\chi)\frac{(\hat{S}_{11}^{(1)}\cos^2\theta + \hat{S}_{12}^{(1)}\sin^2\theta - \hat{S}_{16}^{(1)}\sin\theta\cos\theta)}{\hat{S}_{11}^{(1)} + \chi\hat{S}_{11}^{(2)}}$$

Finally, strain differences are expressed in terms of stresses as

$$\left\{ \begin{matrix} \tilde{\gamma}_{12}^{(1)} - \tilde{\gamma}_{12}^{(2)} \\ \tilde{\varepsilon}_{22}^{(1)} - \tilde{\varepsilon}_{22}^{(2)} \end{matrix} \right\} = -\frac{1}{\chi} \begin{bmatrix} L_{11} & L_{12} \\ L_{21} & L_{22} \end{bmatrix} \left\{ \begin{matrix} \tilde{\sigma}_{12}^{(2)} \\ \tilde{\sigma}_{22}^{(2)} \end{matrix} \right\} + \frac{1}{\chi} \left\{ \begin{matrix} M_1 \\ M_{12} \end{matrix} \right\} \bar{\sigma}_x \tag{31}$$

Here

$$L_{11} = \hat{S}_{66}^{(1)} + a_{12}\hat{S}_{16}^{(1)} + \chi\hat{S}_{66}^{(2)}, \quad L_{12} = \hat{S}_{26}^{(1)} + a_{22}\hat{S}_{16}^{(1)}$$

$$L_{21} = \hat{S}_{26}^{(1)} + a_{12}\hat{S}_{12}^{(1)} + \chi a_{12}\hat{S}_{12}^{(2)}, \quad L_{22} = \hat{S}_{22}^{(1)} + a_{22}\hat{S}_{12}^{(1)} + \chi(\hat{S}_{22}^{(2)} + a_{22}\hat{S}_{12}^{(2)})$$

$$M_1 = (1+\chi)\left[ (\hat{S}_{16}^{(1)} + a_{12}\hat{S}_{11}^{(2)})\cos^2\theta + (\hat{S}_{26}^{(1)} + a_{12}\hat{S}_{12}^{(1)})\sin^2\theta - (\hat{S}_{66}^{(1)} + a_{12}\hat{S}_{16}^{(1)})\sin\theta\cos\theta \right]$$

$$M_2 = (1+\chi)\left[ (\hat{S}_{12}^{(1)} + a_{22}\hat{S}_{11}^{(1)})\cos^2\theta + .(\hat{S}_{22}^{(1)} + a_{22}\hat{S}_{12}^{(1)})\sin^2\theta - (\hat{S}_{26}^{(1)} + a_{22}\hat{S}_{16}^{(1)})\sin\theta\cos\theta \right]$$

Substitution into the equilibrium equations, Eq. (3), yields the following coupled 2nd order differential equations

$$\frac{\mathrm{d}^2}{\mathrm{d}x_2^2} \left\{ \begin{matrix} \tilde{\sigma}_{12}^{(2)} \\ \tilde{\sigma}_{22}^{(2)} \end{matrix} \right\} - \frac{1}{h_1} \begin{bmatrix} K_{11} & K_{12} \\ K_{12} & K_{22} \end{bmatrix} \left( \begin{bmatrix} L_{11} & L_{12} \\ L_{12} & L_{22} \end{bmatrix} \left\{ \begin{matrix} \tilde{\sigma}_{12}^{(2)} \\ \tilde{\sigma}_{22}^{(2)} \end{matrix} \right\} + \left\{ \begin{matrix} M_1 \\ M_2 \end{matrix} \right\} \bar{\sigma}_x \right) = 0 \tag{32}$$

This set of equations is uncoupled at the expense of increasing the order of differentiation, resulting in a fourth order non-homogeneous ordinary differential equation.

## References


1. Highsmith AL, Reifsnider KL (1982) In: Reifsnider KL (eds), Damage in composite materials: mechanisms, accumulation, tolerance, and characterization, ASTM STP 775. ASTM, Philadelphia PA, pp 103–117
2. Bowles DE (1984) J Comp Mater 18(2):173
3. Lundgren JE, Gudmundson P (1999) Comp Sci Technol 59(13):1983
4. Birman V, Byrd L (2001) Comp Part B 31(1):47
5. Nairn JA, Hu S (1992) Intl J Fract 57(1):1–24
6. Bailey JE, Curtis PT, Parvizi A (1979) Proc Roy Soc Lon A A366(1727):599
7. Jamison RD, Schulte K, Reifsnider KL, Stinchcomb WW (1984) In: Wilkins J (ed), Effects of defects in composite materials, ASTM STP 836. ASTM, Philadelphia, PA, pp 21–55
8. Charewicz A, Daniel IM (1986) In: Hahn HT (ed), Composite materials: fatigue and fracture, ASTM STP 907. ASTM, Philadelphia, PA, pp 274–297
9. Kashtalyan M, Soutis C (2002) Int Appl Mech 38(6):641
10. Garrett KW, Bailey JE (1977) J Mater Sci 12(1):157
11. Parvizi A, Garrett KW, Bailey JE (1978) J Mater Sci 13(1):195
12. Daniel IM, Charewicz A (1986) Eng Fract Mech 25(5–6):793
13. Smith PA, Boniface L, Glass NFC (1998) Appl Comp Mater 5(1):11
14. Reifsnider KL, Talug A (1980) Intl J Fatigue 3(1):3
15. Masters JE, Reifsnider KL (1982) In: Reifsnider KL (ed) Damage in composite materials: mechanisms, accumulation, tolerance,

and characterization, ASTM STP 775. ASTM, Philadelphia, PA, pp 40–62
16. O'Brien TK, Hooper SJ (1991) Local delamination in laminates with angle ply matrix cracks: Part I Tension tests and stress analysis. NASA Technical Memorandum 104055/ AVSCOM Technical Report 91-B-010
17. Marsden WM, Guild FJ, Ogin SL, Smith PA (1999) Plastic, Rubber Comp 28(1):30
18. Tong J, Guild FJ, Ogin SL, Smith PA (1997) Comp Sci Technol 57(11):1527
19. Crocker LE, Ogin SL, Smith PA, Hill PS (1997) Comp Part A 28(9–10):839
20. Varna J, Joffe R, Akshantala NV, Talreja R (1999) Comp Sci Technol 59(14):2139
21. Tong J, Guild FJ, Ogin SL, Smith PA (1997) Comp Sci Technol 57(11):1537
22. Lapusta YN, Henaff-Gardin C (2000) Intl J Fract 102(4):L73
23. McCartney LN (1996) In: Proceedings of the 7th European conference on composite materials. London, May
24. Kashtalyan M, Soutis C (2000) Plastics Rubber Comp 29(9):482
25. Zhang J, Herrmann KP (1999) Comp Part A Appl Sci Manufact 30(5):683–706
26. Kashtalyan M, Soutis C (2001) Intl J Fract 112(2):L3
27. Zhang J, Fan J, Soutis C (1992) Composites 23(9):291
28. Jones RM (1999) Mechanics of composite materials, 2nd ed. Francis & Taylor, Philadelphia, PA
29. Mccartney LN (1996) Stress transfer mechanics for ply cracks in general symmetric laminates. NPL Report CMMT(A)50
30. Rikards R, Buchholz FG, Wang H, Bledzki AK, Korjakin A, Richard HA (1998) Eng Fract Mech 61(3–4):325